Journal of Computational Physics 227 (2008) 8254–8267

Contents lists available at ScienceDirect

Journal of Computational Physics

journal homepage: www.elsevier.com/locate/jcp

Local absorbing boundary conditions for elliptical shaped boundaries

M. Medvinsky [a], E. Turkel [a,*], U. Hetmaniuk [b,1]

[a] School of Mathematical Sciences, Tel Aviv University, Ramat Aviv, Tel Aviv 69978, Israel
[b] Sandia National Laboratories, P.O. Box 5800, MS 1320, Albuquerque, NM 87185, United States

ARTICLE INFO

Article history:
Received 24 January 2008
Received in revised form 19 May 2008
Accepted 19 May 2008
Available online 11 July 2008

Keywords:
Helmholtz equation
Absorbing boundary conditions
Mathieu functions

ABSTRACT

We compare several local absorbing boundary conditions for solving the Helmholtz equation, by a finite difference or finite element method, exterior to a general scatterer. These boundary conditions are imposed on an artificial elliptical or prolate spheroid outer surface. In order to compare the computational solution with an analytical solution, we consider, as an example, scattering about an ellipse. We solve the Helmholtz equation with both finite differences and finite elements. We also introduce a new boundary condition for an ellipse based on a modal expansion.

© 2008 Elsevier Inc. All rights reserved.

1. Introduction

We consider scattering exterior to an n-dimensional body based on the Helmholtz equation that describes wave motion in frequency space

$$\begin{aligned} &\Delta u + k^2 u = 0 \text{ exterior to } D,\\ &\text{on } \partial D \qquad u = u^{\text{scat}} + e^{ik\ x\cdot d} \quad \text{(soft body)},\\ &\text{or} \qquad \frac{\partial u}{\partial n} = \frac{\partial}{\partial n}\left(u^{\text{scat}} + e^{ik\ x\cdot d}\right) \quad \text{(hard body)},\\ &\lim_{r\to\infty} r^{\frac{n-1}{2}}\left(\frac{\partial u^{\text{scat}}(x)}{\partial r} - iku^{\text{scat}}(x)\right) = 0 \quad \text{Sommerfeld radiation condition}. \end{aligned} \tag{1}$$

For a numerical solution one needs to truncate the unbounded domain and introduce an artificial surface with a boundary condition to prevent reflections of outgoing waves into the domain. This artificial surface is, in general, convex. We consider local absorbing boundary conditions (ABC) that link only nearby neighbors of a boundary point. Bayliss and Turkel [8] and later with Gunzburger (BGT) [9] constructed a sequence of absorbing boundary conditions, for the wave equation, based on matching terms in an expansion in the inverse radius $\frac{1}{R}$. Since the condition is written in polar coordinates, it is most convenient when the outer surface is a circle or sphere. The most popular is BGT2 which contains a first order normal derivative and a second order tangential derivative and can be easily implemented in both finite differences and finite elements.

When the convex hull of the scatterer is not similar in shape to a circle or a sphere, using an outer surface which is a circle or a sphere artificially enlarges the domain of integration. Such a choice wastes both storage and computer time. For

* Corresponding author.
E-mail addresses: turkel@post.tau.ac.il (E. Turkel), ulhetma@sandia.gov (U. Hetmaniuk).

[1] Sandia National Laboratories is a multiprogram laboratory operated by Sandia Corporation, a Lockheed Martin company, for the United States Department of Energy under Contract DE-AC04-94AL85000.

0021-9991/$ - see front matter © 2008 Elsevier Inc. All rights reserved.
doi:10.1016/j.jcp.2008.05.010

a wave-like equation, this can also aggravate the phase or pollution error [10,39]. When considering boundary conditions imposed directly on the scatterer then one has no choice of the shape of the boundary. We stress that for outer artificial surfaces even though one wishes to minimize the extra points in the domain, nevertheless, one can choose a shape that is convenient computationally and not one that exactly matches the scatterer. Hence, for many objects, such as submarines or other oval-shaped scatterers one can choose the outer surface as an ellipse or a prolate spheroid without excessive waste. This also holds for non-convex scatterers. Many attempts have been made to consider an ABC for general shapes. These have been frequently based either on a series expansion in some generalized radius, or wave number. Other approaches are based on a modal expansion or an approximation to the DtN method. Remarkably, most of these approaches reduced to the BGT condition for a circle or sphere, at least through second order. However, they differ in the boundary condition constructed for other outer shapes. We focus on the case where the outer surface is an ellipse or a prolate spheroid. We compare numerically several approaches. The boundary conditions we compare are those of Grote et al. [19], Reiner et al. [38], Kriegsmann et al. [33], Jones et al. [30], Kallivokas et al. [31,32] and Antoine et al. [2]. In order to compare the computational solution with an analytical solution, we use, as a model problem, scattering about an ellipse. However, the conditions on the outer surface are independent on the shape of the scatterer. Hence, the boundary conditions expressed for an ellipse can be used for scattering about an arbitrary shaped body for which an outer surface of an ellipse is reasonable. Similarly, in three dimensions, one can adapt the various OSRC models for a prolate spheroid to an artificial surface for a volumetric method.

In Section 2, we review several absorbing boundary conditions and comment on their derivation. Then we consider a new ABC for an elliptic outer surface based on a modal expansion in Mathieu functions. We comment on the three-dimensional and time-dependent cases. In Section 3, we compare numerically this new ABC with the other boundary conditions.

2. Absorbing boundary condition (ABC)

The Helmholtz equation exterior to a body is well-posed only if one adds a Sommerfeld radiation condition which gives the behavior of the solution as the domain goes to infinity. To numerically solve the Helmholtz equation, the Sommerfeld radiation condition needs to be replaced by a boundary condition on a surface at a finite distance. For accuracy, this should cause a small change in the global solution. Small is measured relative to the discretization of the interior scheme. Hence, the more accurate the interior solution the greater the need for a more accurate ABC. On the other hand, if the interior approximation is no more than (for example) one percent accurate there is no need for a very accurate absorbing boundary condition. For a given ABC as one refines the grid, the error will decrease according to the order of accuracy of the interior scheme. However, as the grid is further refined this rate will decrease and then level out as the error of the ABC becomes the major component of the total error. If one moves the artificial boundary out the error from the ABC is reduced. However, the error from the interior discretization may increase. Hence, the effect on the total error is unclear.

Several approaches have been suggested for the construction of artificial boundary conditions. One way, pioneered by Engquist and Majda (EM) [17], is to consider waves that enter or leave the domain and to annihilate those scattered waves entering the domain from the outside. The exact boundary condition is a pseudo-differential operator. Engquist and Majda then constructed a sequence of operators, based on a Padé expansion, that are more accurate measured in terms of the angle of incidence to the exterior boundary. Halpern and Trefethen [24] showed that this amounts to constructing a one-way equation that only allows propagation from the interior to the exterior [24]. Higdon [27] and later Ditkowski and Gottlieb [15] have shown that the original Engquist–Majda boundary conditions, when combined with the Helmholtz equation, reduce to the characteristic equation raised to a power.

A different approach is to construct the artificial boundary condition to match a convergent or asymptotic series to the solution where the functional form of the terms is known. The boundary condition is constructed to match the first terms of the outgoing solution. Bayliss and Turkel [8,9] constructed a sequence of such boundary conditions, in a recursive manner, that are more accurate as the distance to the outer boundary increases. One then uses the interior equation to eliminate radial derivatives beyond the first in terms of tangential derivatives. The most popular boundary condition has been BGT2 since this involves only second tangential derivatives. Higher order boundary conditions require higher order tangential derivatives which are not easily implemented with linear finite elements. We shall describe in more detail the Bayliss–Gunzburger–Turkel (BGT2) [9] boundary condition based on an expansion in a polar or spherical radial coordinate.

2.1. Two dimensions

In two dimensions the solution to the exterior Helmholtz equation has a convergent expansion

$$u(r,\theta) = H_0(kr)\sum_{j=0}^{\infty}\frac{F_j(\theta)}{(kr)^j} + H_1(kr)\sum_{j=0}^{\infty}\frac{G_j(\theta)}{(kr)^j}. \tag{2}$$

Instead Bayliss et al. worked with the asymptotic expansion

$$u(r,\theta) \sim \sqrt{\frac{2}{\pi kr}}e^{i(kr-\frac{\pi}{2})}\sum_{j=0}^{\infty}\frac{f_j(\theta)}{(kr)^j}. \tag{3}$$

Matching the two dimensional asymptotic expansion (3) through two terms yields

$$\left(\frac{\partial}{\partial r} - \mathrm{i}k + \frac{5}{2r}\right)\left(\frac{\partial}{\partial r} - \mathrm{i}k + \frac{1}{2r}\right)u = 0 \tag{4}$$

or

$$\frac{\partial^2 u}{\partial r^2} + \left(\frac{3}{r} - 2\mathrm{i}k\right)\frac{\partial u}{\partial r} - \left(k^2 + \frac{3\mathrm{i}k}{r} - \frac{3}{4r^2}\right)u = 0. \tag{5}$$

We now use the Helmholtz equation in polar coordinates

$$\frac{\partial^2 u}{\partial r^2} + \frac{1}{r}\frac{\partial u}{\partial r} + k^2 u + \frac{1}{r^2}\frac{\partial^2 u}{\partial \theta^2} = 0$$

to eliminate $\frac{\partial^2 u}{\partial r^2}$. This yields BGT2

$$\frac{\partial u}{\partial r} = \mathrm{i}ku - \frac{u}{2r} + \frac{u}{8r^2(\frac{1}{r} - \mathrm{i}k)} + \frac{1}{2r^2(\frac{1}{r} - \mathrm{i}k)}\frac{\partial^2 u}{\partial \theta^2}, \tag{6a}$$

$$= \frac{(-\frac{3}{4} + 3\mathrm{i}kr + 2k^2r^2)u + \frac{\partial^2 u}{\partial \theta^2}}{2r^2(\frac{1}{r} - \mathrm{i}k)}. \tag{6b}$$

Expanding this for large kr we find

$$\frac{\partial u}{\partial r} \sim \mathrm{i}k\left[\left(1 + \frac{\mathrm{i}}{2kr} + \frac{1}{8(kr)^2}\right)u + \frac{1}{2(kr)^2}\frac{\partial^2 u}{\partial \theta^2}\right] \quad kr \to \infty. \tag{7}$$

Using instead the full convergent expansion (2) one gets [20,34,25,43]

$$\frac{\partial u}{\partial r} = k\left[\frac{H_0'(kr)}{H_0(kr)}u + \left(\frac{H_0'(kr)}{H_0(kr)} - \frac{H_1'(kr)}{H_1(kr)}\right)\frac{\partial^2 u}{\partial \theta^2}\right], \tag{8}$$

where H is the Hankel function of the first kind. However, $H_0'(z) = -H_1(z)$ and $H_1'(z) = H_0(z) - \frac{1}{z}H_1(z)$. So

$$\frac{\partial u}{\partial r} = -k\left[\frac{H_1(kr)}{H_0(kr)}u + \left(\frac{H_1(kr)}{H_0(kr)} + \frac{H_0(kr)}{H_1(kr)} - \frac{1}{kr}\right)\frac{\partial^2 u}{\partial \theta^2}\right]. \tag{9}$$

Using the asymptotic properties of the Hankel functions for large argument the modal expansion agrees with BGT2 (7) through $\mathrm{O}\left(\frac{1}{(kr)^2}\right)$ for large kr. For high frequencies it is more convenient to use (6a). For low frequencies it is necessary to use (8), see [43] for more details. For scattering problems [39,1] have shown that BGT is more accurate than EM. Matching more terms in the expansion does not guarantee that the result is more accurate. However, [9,21,23,18,26] provide theorems that provide stability and error bounds for some cases.

When the outer surface is not a circle or sphere there are several approaches to generalize the BGT boundary conditions. One is to use a change of variables and the chain rule to express the r and θ derivatives in terms of normal and tangential derivatives in (6a), (8) to the given outer surface [34–36]. When the outer surface is given analytically an alternative approach is to rederive the formula based on an expansion for the solution of the Helmholtz equation in terms of coordinates that give the outer surface to replace BGT2. Another approach is to derive a global formula which couples all the points on the boundary. One then approximates the integral to get a local boundary condition. This again gives the BGT formula, for a circle, in terms of the normal and tangential directions [19,20,25]. If the outer surface is an ellipse then the first approach converts (r, θ) derivatives to elliptical coordinates. The second approach derives an asymptotic expansion in terms of elliptical coordinates and then matches this expansion. For the infinite series the two approaches are the same. However, since we use only a finite number of terms (usually two) the two approaches differ. In the first approach the assumption is that the solution is well represented by a few circular waves and this is transformed to elliptical coordinates. In the second approach the assumption is that the solution is well approximated by the first two elliptical waves. Since these are based on the outer surface shape rather than the scatterer neither approach is really correct. However, under the assumption that the shape of the outer surface matches closely the shape of the scatterer it would seem that the second approach would be more accurate.

We present several extensions of the BGT boundary conditions to more general shapes. Some of these are general and some refer only to elliptical outer boundaries. An ellipse, $\xi = \xi_0$, with semi-major and semi-minor axes a and b respectively is given parametrically by

$$x = a\cos(\eta) = f\cosh(\xi_0)\cos(\eta) \quad y = b\sin(\eta) = f\sinh(\xi_0)\sin(\eta) \tag{10a}$$

$$f = a^2 - b^2. \tag{10b}$$

Defining $h_\xi = h_\eta = \frac{\partial s}{\partial \eta}$, we have

$$h_\xi = f\sqrt{\cosh^2(\xi) - \cos^2(\eta)} \overset{\text{on ellipse}}{\rightarrow} \sqrt{a^2 - f^2\cos^2(\eta)} = \sqrt{a^2\sin^2(\eta) + b^2\cos^2(\eta)}$$

and

$$\frac{\partial u}{\partial n} = \frac{1}{h_\xi}\frac{\partial u}{\partial \xi} \quad \frac{\partial u}{\partial s} = \frac{1}{h_\xi}\frac{\partial u}{\partial \eta}.$$

The Helmholtz equation, in elliptical coordinates, is given by

$$\frac{\partial^2 u}{\partial \xi^2} + \frac{\partial^2 u}{\partial \eta^2} + h_\xi^2 k^2 u = 0 \tag{11}$$

and the curvature of the ellipse is given by

$$\kappa = \frac{ab}{h_\xi^3}.$$

Grote and Keller [19] and later Thompson, Huan and Ianculescu [42] found that for an ellipse, using an expansion in Mathieu functions, coupled with a DtN formula the BGT2 condition remains with r replaced by the ellipse-radius $f\cosh(\xi)$. This was also discovered at the same time by Ben-Porat and Givoli [11]. It yields at the ellipse $\xi = \xi_0$

$$\frac{\partial^2 u}{\partial \xi^2} + \alpha\frac{\partial u}{\partial \xi} + \beta u = 0 \tag{12}$$

with (using $a = f\cosh(\xi_0), b = f\sinh(\xi_0)$)

$$\alpha = 3\tanh(\xi_0) - 2ikf\sinh(\xi_0) - \coth(\xi_0) = 3\frac{b}{a} - 2ikb - \frac{a}{b},$$
$$\beta = \frac{3}{4}\tanh^2(\xi_0) - (kf\sinh(\xi_0))^2 - 3ikf\sinh(\xi_0)\tanh(\xi_0) = \frac{3}{4}\frac{b^2}{a^2} - k^2b^2 - 3ik\frac{b^2}{a}.$$

They [42] used the Helmholtz equation in elliptical coordinates to eliminate the $\frac{\partial^2 u}{\partial \xi^2}$ derivative. This gives

$$\frac{\partial u}{\partial \xi} = \frac{1}{\alpha}\left((k^2h_\xi^2 - \beta)u + \frac{\partial^2 u}{\partial \eta^2}\right). \tag{13}$$

Reiner et al. [38] considered an extension of BGT2 for an ellipse based on the condition of Grote and Keller [19]. They used the Helmholtz equation in polar coordinates to eliminate the second radial derivative substituting $r \to f\cosh(\xi)$. They developed the ABC

$$\frac{\partial u}{\partial \xi} = \frac{b}{a}\left[\left(ika - \frac{1}{2} + \frac{1}{8(1-ika)}\right)u + \frac{1}{2(1-ika)}\frac{\partial^2 u}{\partial \eta^2}\right]. \tag{14}$$

The first to consider more general shapes for the outer boundary was Kriegsmann et al. [33]. They considered the BGT formula for the circle (6a) and formally replaced $\frac{\partial}{\partial r} \to \frac{\partial}{\partial n}$, $\frac{1}{r} \to \kappa$ where κ is the curvature and $\frac{1}{r^2}\frac{\partial^2 u}{\partial \theta^2} \to \frac{\partial^2 u}{\partial s^2}$. So they arrived at the boundary condition

$$\frac{\partial u}{\partial n} = iku - \frac{\kappa u}{2} - \frac{\kappa^2 u}{8(ik-\kappa)} - \frac{1}{2(ik-\kappa)}\frac{\partial^2 u}{\partial s^2}. \tag{15}$$

Since $\kappa = \kappa(s)$ this is not in symmetric form. To recover a symmetric form, Antoine [3] suggested replacing (15) with

$$\frac{\partial u}{\partial n} = iku - \frac{\kappa u}{2} - \frac{\kappa^2 u}{8(ik-\kappa)} - \frac{\partial}{\partial s}\left(\frac{1}{2(ik-\kappa)}\frac{\partial u}{\partial s}\right). \tag{16}$$

Since Kriegsmann et al. developed (15) purely formally, (16) is just as legitimate as (15). Antoine [3] has shown that for a finite element method the symmetric form is more accurate. Later Jones [28–30] suggested including derivatives of the curvature

$$\frac{\partial u}{\partial n} = iku - \frac{\kappa u}{2} - \frac{\kappa^2 u}{8(ik-\kappa)} - \frac{1}{2(ik-\kappa)}\frac{\partial^2 u}{\partial s^2} + \frac{ik}{ik-\kappa}\left[\frac{1}{8k^2}\frac{d^2\kappa}{ds^2}u + \frac{1}{2k^2}\frac{\partial \kappa}{\partial s}\frac{\partial u}{\partial s}\right] \tag{17}$$

which is not in symmetric form. As was done with (15), (16), we obtain a symmetric form by replacing it with

$$\frac{\partial u}{\partial n} = \left(ik - \frac{\kappa}{2} - \frac{\kappa^2}{8(ik-\kappa)} - \frac{1}{8ik(ik-\kappa)}\frac{d^2\kappa}{ds^2}\right)u - \frac{\partial}{\partial s}\left(\frac{1}{2(ik-\kappa)}\frac{\partial u}{\partial s}\right). \tag{18}$$

Antoine et al. [2] considering a decomposition into incoming and outgoing wave constructed, based on pseudo-differential operators, an asymptotic expansion in $\frac{1}{k}$ for general bodies. For the two terms that they calculated, they recovered the BGT boundary condition for the circle and the sphere. For general two dimensional shapes they derived a full second order operator

$$\frac{\partial u}{\partial n} = \mathrm{i}ku - \frac{\kappa u}{2} - \frac{\kappa^2 u}{8(\mathrm{i}k-\kappa)} + \frac{1}{8k^2}\frac{\mathrm{d}^2\kappa}{\mathrm{d}s^2}u - \frac{\partial}{\partial s}\left(\frac{1}{2(\mathrm{i}k-\kappa)}\frac{\partial u}{\partial s}\right). \tag{19}$$

Kallivokas et al. [31,32] considered a geometric optics type expansion and developed a second order absorbing boundary condition

$$\begin{aligned}\frac{\partial u}{\partial n} &= \mathrm{i}ku - \frac{\kappa u}{2} - \frac{1}{2(\mathrm{i}k-\kappa)}\left(\frac{\partial^2 u}{\partial s^2} + \frac{1}{4}\kappa^2 u\right) - \frac{1}{2(\mathrm{i}k-\kappa)^2}\left[\frac{1}{4}\frac{\mathrm{d}^2\kappa}{\mathrm{d}s^2}u + \frac{\mathrm{d}\kappa}{\mathrm{d}s}\frac{\partial u}{\partial s}\right] \\ &= \left(\mathrm{i}k - \frac{\kappa}{2} - \frac{\kappa^2}{8(\mathrm{i}k-\kappa)} - \frac{1}{8(\mathrm{i}k-\kappa)^2}\frac{\mathrm{d}^2\kappa}{\mathrm{d}s^2}\right)u - \frac{\partial}{\partial s}\left(\frac{1}{2(\mathrm{i}k-\kappa)}\frac{\partial u}{\partial s}\right).\end{aligned} \tag{20}$$

The difference between these formulae and the modified Kriegsmann et al. (16) and modified Jones (18) is the coefficient of the term $\frac{\mathrm{d}^2\kappa}{\mathrm{d}s^2}u$. The coefficient is $-\frac{1}{8\mathrm{i}k(\mathrm{i}k-\kappa)}$ in (18), $\frac{1}{8k^2}$ in (19), $-\frac{1}{8(\mathrm{i}k-\kappa)^2}$ in (20) and does not appear in (16). Hence, for large k (relative to the curvature) all these methods are similar. For small k the boundary condition of Antoine et al. becomes infinite and less accurate. For intermediate wave numbers it is not obvious how they compare.

Another approach is to use the BGT2 condition. Then r and θ derivatives are converted to elliptical derivatives using the chain rule. This leads to a complicated formula. Furthermore a mixed second derivative now appears. Ways of treating this are discussed in [35]. This approach was tried with the finite difference formula without great success and will not be pursued further. This approach is used in [44] to develop a BGT2 type formula for Cartesian coordinates.

We have given numerous alternatives for the absorbing boundary condition on the artificial boundary both for ellipses and for general shapes. These boundary conditions are derived based on different assumptions: asymptotic expansions in a reciprocal elliptical distance, an expansion for large wavenumbers, a geometric optics expansion and finally a change of variables from the BGT2 formula. Some of these conditions account for the non-constant curvature of the ellipse while others do not include such terms. However, the validity of the underlying expansion does not guarantee that this leads to an accurate solution, i.e. replacing the Sommerfeld condition at infinity by these conditions at a finite distance leads to a small error in the numerical solution. There is a paucity of comparisons between these options [14].

In this study we concentrate on absorbing boundary conditions on an outer artificial surface for a volume discretization such as finite difference (FD) or finite element methods (FEM). Another approach introduced by Kriegsmann et al. [33] is to specify these conditions on the scatterer itself (OSRC). Some extensions to high frequency problems are given in [12,13,4]. Higher order extension of radiation conditions are examined in [40,45]. A survey of these techniques is given in [5]. A comparison of several of these OSRC boundary conditions is presented in [37]. As seen above any condition derived as an OSRC can also be applied as an ABC on an artificial bounding surface for a volume method.

2.2. New absorbing boundary condition

In elliptical coordinates (10a) the Helmholtz equation is given by (11)

$$\frac{\partial^2 u}{\partial \xi^2} + \frac{\partial^2 u}{\partial \eta^2} + \frac{k^2 f^2}{2}(\cosh(2\xi) - \cos(2\eta))u = 0. \tag{21}$$

Assume $u = \psi(\xi)\lambda(\eta)$. Then

$$\begin{cases} \frac{\mathrm{d}^2\psi}{\mathrm{d}\xi^2} + \left(\frac{k^2 f^2}{2}\cosh(2\xi) - l\right)\psi = 0, \\ \frac{\mathrm{d}^2\lambda}{\mathrm{d}\eta^2} - \left(\frac{k^2 f^2}{2}\cos(2\eta) - l\right)\psi = 0. \end{cases} \tag{22}$$

l is separation constant determined so that $\lambda(\eta)$ is periodic which leads to either even or odd solutions with eigenvalues $l_r(q)$ for r even, where q is given by

$$q = \frac{k^2 f^2}{4} = \frac{k^2}{4}\left(a^2 - b^2\right). \tag{23}$$

It is not clear which Mathieu functions to choose as the first two functions ψ_i. The ones with the lowest characteristic values are the first even and then the first odd Hankel-like Mathieu function. However, the exact solution for scattering about an ellipse with a plane wave at zero angle does not contain any of the odd Mathieu functions (by symmetry). Also, for larger aspect ratios the first even and the first odd characteristic values are extremely close. Hence, we choose the first two even Mathieu–Hankel functions, $M_0(\xi), M_1(\xi)$ with the corresponding characteristic values l_0, l_1.

We assume an expansion in functions [34]

$$u(\xi,\eta) = \lambda_0(\eta)M_0(\xi) + \lambda_1(\eta)M_1(\xi), \tag{24a}$$

$$\frac{\partial u}{\partial \xi}(\xi,\eta) = \lambda_0(\eta)M_0'(\xi) + \lambda_1(\eta)M_1'(\xi), \tag{24b}$$

$$\frac{\partial^2 u}{\partial \xi^2}(\xi,\eta) = \lambda_0(\eta)M_0''(\xi) + \lambda_1(\eta)M_1''(\xi). \tag{24c}$$

Solving for λ_0 and λ_1 at $\xi = \xi_0$ from the first two equations we get

$$\lambda_0 = \left.\frac{M_1' u - M_1 \frac{\partial u}{\partial \xi}}{(M_0 M_1' - M_0' M_1)}\right|_{\xi=\xi_0} \qquad \lambda_1 = -\left.\frac{M_0' u - M_0 \frac{\partial u}{\partial \xi}}{(M_0 M_1' - M_0' M_1)}\right|_{\xi=\xi_0}.$$

Substituting in (24c) one gets

$$\frac{\partial^2 u}{\partial \xi^2} + \frac{M_1 M_0'' - M_0 M_1''}{M_0 M_1' - M_0' M_1}\frac{\partial u}{\partial \xi} + \frac{(-M_1' M_0'' + M_0' M_1'')}{M_0 M_1' - M_0' M_1} u = 0. \tag{25}$$

Define

$$D = M_0 M_1' - M_1 M_0' \quad T = -\frac{D}{(l_1 - l_0)M_0 M_1} = \frac{\frac{M_0'}{M_0} - \frac{M_1'}{M_1}}{l_1 - l_0}.$$

D is a Wronskian of linearly independent solutions and so nonzero.

We note that T is a function of ξ but not η. Using (25) and (22) for M_0'' and M_1'', we get

$$\frac{\partial^2 u}{\partial \xi^2} - \frac{(l_1 - l_0)M_0 M_1}{D}\frac{\partial u}{\partial \xi} + \left(2q\cosh(2\xi) - l_0 + \frac{(l_1 - l_0)M_0' M_1}{D}\right)u = 0. \tag{26}$$

We use the Helmholtz equation to eliminate $\frac{\partial^2 u}{\partial \xi^2}$ in terms of $\frac{\partial^2 u}{\partial \eta^2}$. Subtracting (21) from (26) we get

$$\frac{\partial u}{\partial \xi} = T\frac{\partial^2 u}{\partial \eta^2} + \left(T(l_0 - 2q\cos(2\eta)) + \frac{M_0'}{M_0}\right)u. \tag{27}$$

For a slightly different approach see [7]. When coupling this condition with a finite element discretization of the Helmholtz equation the resulting linear system will be complex symmetric.

2.3. Three dimensions

In three dimensions there is a convergent series given by

$$u(r,\theta,\phi) = \frac{e^{ikr}}{kr}\sum_{j=0}^{\infty}\frac{f_j(\theta,\phi)}{(kr)^j}. \tag{28}$$

For three dimensions, the BGT2 absorbing boundary condition becomes

$$\frac{\partial u}{\partial r} = (ik - \frac{1}{r})u + \frac{1}{2r(1 - ikr)}\Delta_s u, \tag{29}$$

where Δ_s is the Laplace–Beltrami operator given in spherical coordinates by

$$\Delta_s u = \frac{1}{\sin(\phi)}\frac{\partial}{\partial \phi}\left(\sin(\phi)\frac{\partial u}{\partial \phi}\right) + \frac{1}{\sin^2(\phi)}\frac{\partial^2 u}{\partial \theta^2}.$$

Similar to (8) one can derive an absorbing boundary condition in terms of spherical Hankel functions. Since these reduce to polynomials for an integer index this boundary condition is identical to (29) [20,25].

For three dimensions, Jones [28] derived

$$\frac{\partial u}{\partial n} = (ik - \mathscr{H})u - \frac{i}{2k}(\mathscr{K} - \mathscr{H}^2)u - \mathrm{div}_\Gamma\left(\frac{1}{2ik}(\mathscr{I} - \frac{i\mathscr{R}}{k})\nabla_\Gamma\right)u. \tag{30}$$

Using an expansion in k, based on pseudo-differential operators, Antoine et al. [2] derived

$$\frac{\partial u}{\partial n} = (ik - \mathscr{H})u + \frac{1}{2}(ik - 2\mathscr{H})^{-1}(\mathscr{K} - \mathscr{H}^2)u + \frac{\Delta_\Gamma \mathscr{H}}{4k^2}u - \mathrm{div}_\Gamma\left(\frac{1}{2}(ik\mathscr{I} - \mathscr{R})^{-1}\nabla_\Gamma\right)u. \tag{31}$$

To recover the three dimensional generalization of Kriegsmann et al., we would eliminate the term $\frac{\Delta_\Gamma \mathscr{H}}{4k^2}u$. In these formulae Δ_Γ is the Laplace–Beltrami operator on the surface Γ, $\nabla_\Gamma v$ denotes the surface divergence of the tangential vector field v, $\mathscr{H} = \frac{\kappa_1 + \kappa_2}{2}$ is the mean curvature, $\mathscr{K} = \kappa_1\kappa_2$ is the Gaussian curvature where κ_1 and κ_2 are the principal curvatures and $\mathscr{R}$

is the curvature tensor. The two dimensional and three dimensional absorbing boundary conditions of Antoine et al. have been implemented in a finite element code for wave scattering about submarine-like bodies in [16,41] respectively. Based on an analogy with the two dimensional case the boundary condition of Kallivokas et al. [31] would be the same as (31) except that the term $\frac{\Delta_\Gamma \mathscr{H}}{4k^2}u$ is replaced by $\frac{1}{4k^2}(1-\frac{2\mathscr{H}}{\mathrm{i}k})^{-2}\Delta_\Gamma \mathscr{H}\cdot u$.

In order to compare the boundary conditions of Jones (30) and Antoine (31), we approximate the boundary condition of Antoine (31) using $\frac{1}{1-\epsilon}=1+\epsilon+\mathrm{O}(\epsilon)^2$. Then (31) becomes

$$\frac{\partial u}{\partial n}=(\mathrm{i}k-\mathscr{H})u+\frac{1}{2\mathrm{i}k}\left(1+\frac{2\mathscr{H}}{\mathrm{i}k}\right)(\mathscr{K}-\mathscr{H}^2)u+\frac{\Delta_\Gamma \mathscr{H}}{4k^2}u-\mathrm{div}_\Gamma\left(\frac{1}{2\mathrm{i}k}(\mathscr{I}+\frac{\mathscr{R}}{\mathrm{i}k})\nabla_\Gamma\right)u$$

or

$$\frac{\partial u}{\partial n}=(\mathrm{i}k-\mathscr{H})u+\frac{1}{2\mathrm{i}k}((\mathscr{K}-\mathscr{H}^2)u-\Delta_\Gamma u)+\frac{1}{k^2}\left[\mathscr{H}(\mathscr{H}^2-\mathscr{K})u+\frac{1}{4}\Delta_\Gamma \mathscr{H}u+\frac{1}{4}\mathrm{div}_\Gamma(\mathscr{R}\nabla_\Gamma u)\right]. \tag{32}$$

We see that (30) and (32) agree through the $\frac{1}{\mathrm{i}k}$ terms with some differences in the $\frac{1}{k^2}$ terms just as occurred in two dimensions. The paper of Antoine et al. [2] gives a mathematical justification for many of these techniques.

To derive the modal expansion approximation in three dimensions we again consider (25). We now replace M_j by the first two (prolate) spheroidal-Hankel functions and use the Helmholtz equation in spheroidal coordinates to eliminate $\frac{\partial^2 u}{\partial \xi^2}$. For a slightly different approach see [6].

2.4. Time dependent problems

In this section, we consider the wave equation

$$\frac{\partial^2 v}{\partial t^2}=c^2\Delta v. \tag{33}$$

This is converted to the Helmholtz equation by assuming that $v(\mathbf{x},t)=\mathrm{e}^{-\mathrm{i}\omega t}u(\mathbf{x})$ and defining $k=\frac{\omega}{c}$. Time derivatives are replaced by multiplication by $-\mathrm{i}\omega$. So any local absorbing boundary condition for the Helmholtz equation that is non-conservative form and has coefficients that are a rational function of $\mathrm{i}k$ can be converted to a local boundary condition for the wave equation by multiplying to remove the denominators. When the boundary condition is in divergence-free form this can not be done directly since the coefficient is inside the space derivative. Instead we introduce auxiliary variables.

As an example, consider the formula of Kallivokas et al. (20). Define $v=\frac{1}{\mathrm{i}k-\kappa}\frac{\partial u}{\partial s}$. Then (20) can be rewritten as the system

$$(\mathrm{i}k-\kappa)^2\frac{\partial u}{\partial n}=\left((\mathrm{i}k-\frac{\kappa}{2})(\mathrm{i}k-\kappa)-\frac{\kappa^2}{8}\right)(\mathrm{i}k-\kappa)u-\frac{1}{8}\frac{d^2\kappa}{ds^2}u-\frac{(\mathrm{i}k-\kappa)^2}{2}\frac{\partial v}{\partial s}$$

$$(\mathrm{i}k-\kappa)v=\frac{\partial u}{\partial s}.$$

This can then be transformed by $\mathrm{i}k\to\frac{1}{c}\frac{\partial}{\partial t}$. Auxiliary variables have previously been used to implement higher order absorbing boundary conditions, see, e.g. [22,32]. The boundary condition of Kriegsmann et al. (15) is much easier to transform to the time domain. It can be written as

$$\left(\frac{1}{c}\frac{\partial}{\partial t}-\kappa\right)\frac{\partial u}{\partial n}=\left(\frac{1}{c^2}\frac{\partial^2}{\partial t^2}-\frac{3\kappa}{2c}\frac{\partial}{\partial t}+\frac{3\kappa^2}{8}\right)u-\frac{1}{2}\frac{\partial^2 u}{\partial s^2}.$$

From the result section this boundary is the best at least for ellipses. It is well known that the behavior for long times is determined by the behavior for low frequencies, see, e.g. [21]. In two dimensions, we found that BGT2 does not converge as the frequency goes to zero. The modal expansion in Hankel functions has a small error for low frequencies in scattering about a circle. Similarly for scattering about an ellipse, the expansion in Mathieu functions was the only one that has a small error for small k. However, both the Hankel functions and the Mathieu functions are not rational functions of their argument. Hence, there is no local way to convert the boundary condition (8) to the time domain rather this is equivalent to a global boundary condition in time. In three dimensions the expansion in spherical Hankel functions is identical to BGT2. As seen in the results, BGT2 indeed is reasonable for low frequencies in three dimensions. In this case the error is frequency independent (i.e. constant) as k goes to zero for a given scatterer.

Though this does not consist of a proof, nevertheless it indicates that for the wave equation in two space dimensions there is no local in time boundary condition that converges for long time. However, for three space dimensions the time dependent BGT2 [8] might be well behaved even for long times. For a more detailed discussion of long term stability for BGT see [21].

3. Results

We first consider scattering by a plane wave about a circle and sphere. We solve the scattering problem with a Dirichlet boundary condition. The Helmholtz equation is solved by a finite element method with linear rectangular elements in polar/spherical coordinates (independent of ϕ). The inner circle has radius 1 and the outer circle has radius 2.

We study the effect of the absorbing boundary condition on the relative error of the far field pattern. In particular, in two dimensions, we compare the error due to the standard BGT boundary condition (6) with the improvement based on the Hankel expansion (8). We change the number of elements in the radial and angular direction. We use 180 samples for the far-field pattern (FFP), uniformly distributed in $[0, 2\pi]$. We display the relative error

$$\sqrt{\frac{\sum_i |\,\mathrm{FFP}_{\mathrm{comp}}(\theta_i) - \mathrm{FFP}_{\mathrm{exact}}(\theta_i)|^2}{\sum_i |\,\mathrm{FFP}_{\mathrm{exact}}(\theta_i)|^2}}.$$

We also display the error in the FFP for three dimensional scattering about a sphere.

Comparing the columns of Table 1, we see that BGT2, in two dimensions, is slightly more accurate than the Hankel boundary condition for $k = 2$. However, for lower wave numbers the modal boundary condition is better. For very low wave numbers the BGT2 boundary condition diverges while the Hankel boundary condition gives excellent results, even improving slowly as the wavenumber goes to zero. The BGT2 error on the fine meshes (40×240 and 120×720) is due to the absorbing boundary condition while with Hankel boundary condition, the error for $k \leqslant 0.1$ is dominated by the finite element error. To keep the same level of error as k increases, we need finer meshes. However, in these experiments, we are not trying to keep the same level of error but to assess the error due to the absorbing boundary condition. The error due to the ABC is decreasing as k decreases. So we need a smaller error from the FEM discretization to assess the error due to the ABC which results in finer meshes for smaller k. We note that for $k = 0$ the modal boundary condition (9) is singular and one would need L'Hospital's rule to evaluate it. Furthermore, for the Laplace equation the Sommerfeld radiation condition is replaced by boundedness at infinity.

We next solve the scattering problem by a sphere with a Dirichlet boundary condition. The inner sphere has radius 1 and the outer sphere has radius 2. We use linear Q1 elements in spherical coordinates. The problem is independent of ϕ. We change the number of elements in the radial and angular direction. We use 90 samples for the far-field pattern, uniformly distributed in $[0, \pi]$. As before, Table 2 gives the relative error in the far field pattern. The error due to the ABC is decreasing as k decreases. The relative error for the FFP for $k \leqslant 0.1$ is still dominated by the finite element discretization error.

We now consider the problem exterior to an ellipse solved with a finite difference method in elliptical coordinates. The scatterer and outer artificial surface are concentric ellipses with semi-major axis 1 for the scatterer. The minor axis for the outer surface is determined so that the inner and outer ellipses have the same f, (10b). The mesh is 150 (radial–elliptical) by 180 (polar–elliptical) nodes. Finer meshes were also used to verify the results were independent of the interior mesh. For the ABC of Kriegsmann et al. and Jones the original nonsymmetric version (15) and (17) was implemented. The tangential derivatives were rewritten in ξ, ϕ coordinates and the curvature term was the analytical value for an ellipse. We compare the solutions when the outer ellipse has a semi-major axis of 1.1 or 1.5. We see a great improvement when the outer surface is not extremely close to the scatterer. In Tables 3 and 4 we compare several schemes with an aspect ratio of 2 and Dirichlet or Neumann conditions on the scatterer respectively. The L_2 error is then computed on the other, non-specified, portion of

Table 1
FFP relative error for 2D problem with BGT2

k	Mesh 40×240		Mesh 120×720	
	BGT2	Hankel ABC	BGT2	Hankel ABC
2	8.076×10^{-4}	1.272×10^{-3}	8.278×10^{-4}	1.264×10^{-3}
1	2.231×10^{-3}	4.983×10^{-4}	2.2387×10^{-3}	4.863×10^{-4}
.1	1.465×10^{-1}	6.657×10^{-6}	1.465×10^{-1}	8.107×10^{-7}
.01	5.860×10^{-1}	3.922×10^{-6}	5.859×10^{-1}	4.358×10^{-7}
.001	1.185	2.713×10^{-6}	1.185	3.015×10^{-7}
.0001	1.836	2.065×10^{-6}	1.836	2.295×10^{-7}
.00001	2.505	1.664×10^{-6}	2.505	1.849×10^{-7}

Table 2
FFP relative error for 3D problem with BGT2

k	Mesh 10×60	Mesh 40×240	Mesh 120×720
2	3.234×10^{-3}	1.188×10^{-3}	1.237×10^{-3}
1	1.410×10^{-3}	2.822×10^{-4}	2.491×10^{-4}
.1	9.665×10^{-4}	6.061×10^{-5}	6.747×10^{-6}
.01	9.689×10^{-4}	6.075×10^{-5}	6.752×10^{-6}
.001	9.689×10^{-4}	6.075×10^{-5}	6.751×10^{-6}
.0001	9.689×10^{-4}	6.075×10^{-5}	6.751×10^{-6}
.00001	9.689×10^{-4}	6.075×10^{-5}	6.751×10^{-6}

the normalized trace. In Fig. 1 we compare all the boundary conditions for an ellipse with aspect ratio 2 and $k = 1$. The two subfigures are when the outer surface has a major semi-axis 1.1 and 1.5. In Fig. 2 we repeat the computation but with an aspect ratio of 10. Finally, in Fig. 3 we consider an aspect ratio of 2 with wavenumber $k = 4$. The new ABC based on a modal expansion in Mathieu functions, (27), is the best. Among the standard ABCs, that of Grote and Keller (13), Jones (17), and Kriegsmann et al. (15) were next best. The ABC of Kriegsmann (15) eliminates the derivative of the curvature and so this and the Grote and Keller scheme are easy to implement. For higher wavenumbers most of the boundary conditions yield similar accuracy.

To gain an overview of the impact of the parameters, we compare the new modal boundary condition for various parameters when a Neumann boundary condition is specified on the scatterer. For the comparison, we choose the ABC of Kriegsmann (15) as a typical and good ABC. We also include the conditions of Jones (17) and Grote and Keller (13). We first compare them, in Fig. 4(a), as a function of k, for fixed aspect ratio and fixed outer radius. In Fig. 4(b) we fix $k = 1$ and an aspect ratio of 2 and see the effect of the position of the outer boundary. In Fig. 5(a), we fix $k = 1$ and the position of the outer boundary ($a = 1.5$) and plot the effect of varying the aspect ratio of the scatterer. Finally, in Fig. 5(b), we fix $k = 1$, $a = 1.5$, and an aspect ratio ellipse of 2 and plot the effect of varying the angle of incidence. We see that the angle of incidence has a small effect on the accuracy of the absorbing boundary conditions. In all cases the modal boundary condition is best or close to the best.

Table 3
FD Dirichlet bc, L_2 errors of normalized boundary normal derivative

AR = 2	$k = 0.5$	$k = 1$	$k = 2$	$k = 4$
Kriegsmann	0.018	0.015	0.009	0.012
Jones	0.016	0.012	0.008	0.012
Antoine	0.037	0.017	0.009	0.012
Kallivokas	0.022	0.015	0.012	0.017
Reiner	0.059	0.038	0.042	0.040
Grote	0.011	0.008	0.008	0.011
Mathieu	0.006	0.007	0.008	0.011

Table 4
FD Neumann bc, L_2 errors of normalized boundary solution

AR = 2	$k = 1$	$k = 2$	$k = 3$	$k = 4$
Kriegsmann	0.012	0.008	0.005	0.007
Jones	0.010	0.006	0.005	0.007
Antoine	0.022	0.009	0.006	0.007
Kallivokas	0.014	0.007	0.007	0.015
Reiner	0.040	0.036	0.048	0.037
Grote	0.015	0.004	0.005	0.005
Mathieu	0.006	0.003	0.005	0.006

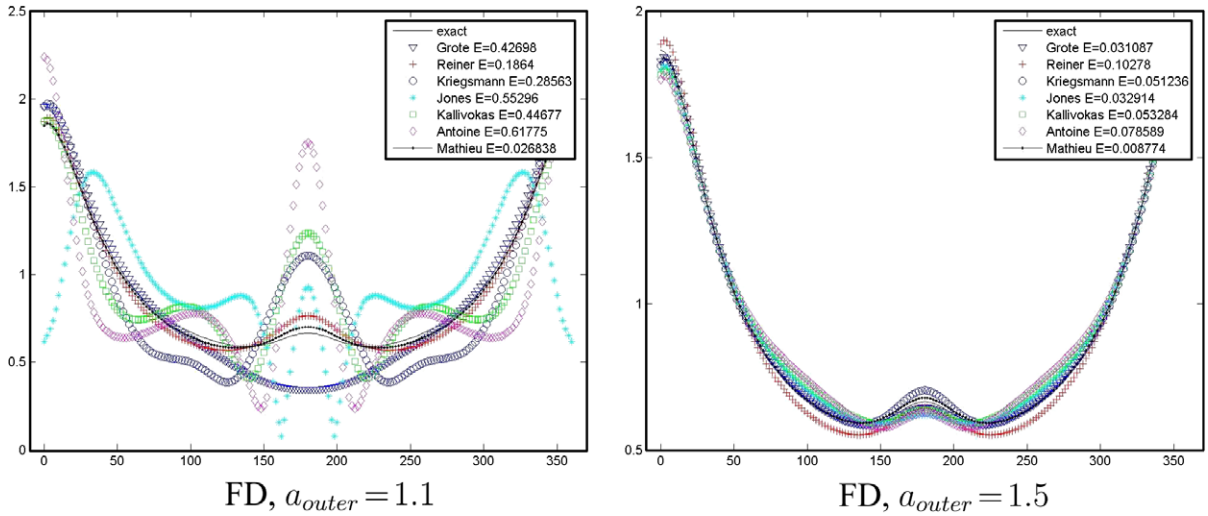

Fig. 1. L_2 error, Dirichlet bc, $k = 1$, aspect-ratio-ellipse (AR) = 2.

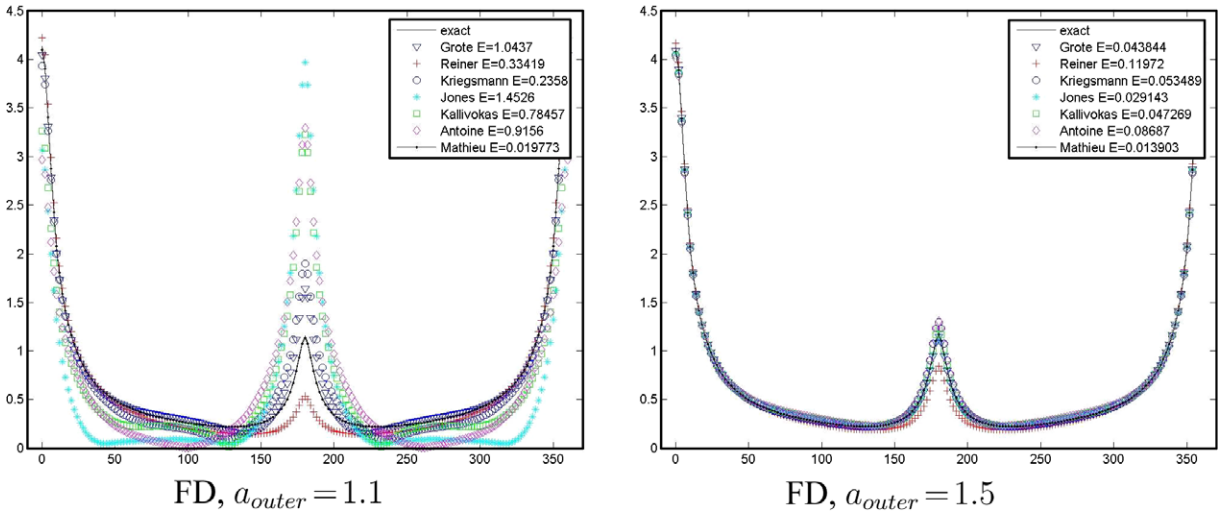

Fig. 2. L_2 error, Dirichlet bc, $k = 1$, AR = 10.

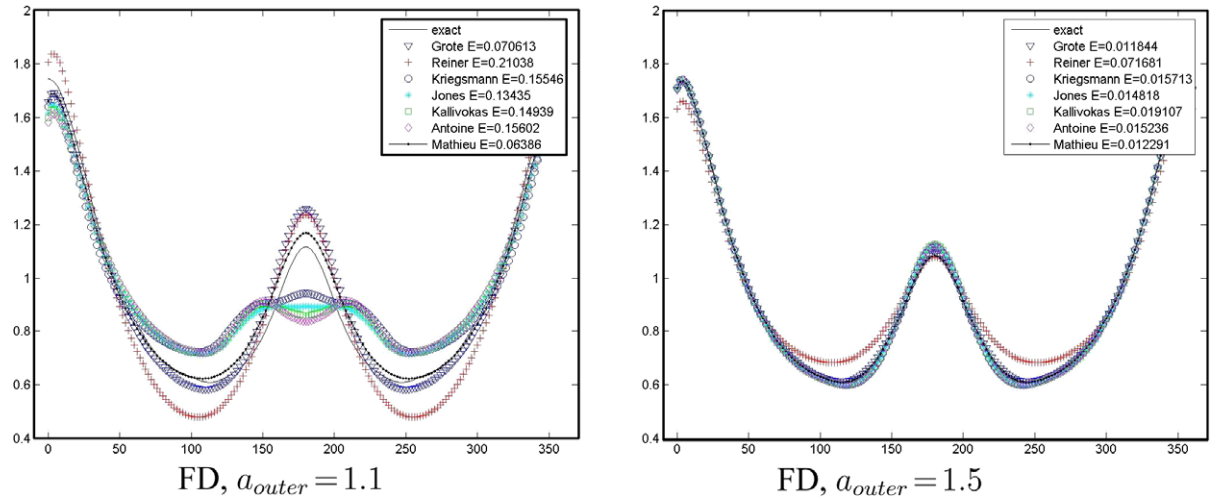

Fig. 3. L_2 error, Dirichlet bc, $k = 4$, AR = 2.

We now implement a linear finite element code exterior to a hard (natural boundary condition) elliptical scatterer. We consider plane wave scattering at 0° angle of incidence. The scatterer has a semi-major axis $a = 1$ with the semi-minor axis given. For the outer surface we specify the semi-major axis and the semi-minor axis is determined so that f (10b) is the same as for the scatterer. A 50×200 quadrilateral mesh in polar coordinates is used to minimize the discretization error. For $k = 4$ a 60×600 mesh is used. The aspect ratio of the scatterer is given in the tables. In these comparisons, we use the following ABCs: Kriegsmann (16), Jones (18), Antoine (19), Kallivokas (20), Reiner (14), Grote (13), and the modal expansion (27). Now the bc of Kriegsmann et al. and Jones are the symmetric versions.

We consider an ellipse with aspect ratio 2. The outer ellipse has a semi-major axis of 1.5. In Table 5, we show the error in u on the inner boundary

$$\left\| \frac{\mathbf{u}_{\text{ex}}}{\|\mathbf{u}_{\text{ex}}\|} - \frac{\mathbf{u}_{\text{fem}}}{\|\mathbf{u}_{\text{fem}}\|} \right\|_2$$

while in Table 6, we report the error in the far field pattern (FFP)

$$\left\| \frac{\text{FFP}_{\text{ex}}}{\|\text{FFP}_{\text{ex}}\|} - \frac{\text{FFP}_{\text{fem}}}{\|\text{FFP}_{\text{fem}}\|} \right\|_2.$$

In Table 7, we redo the calculation with the outer artificial ellipse brought in closer to a semi-major axis of 1.1. In Table 8 we consider an ellipse with a high aspect ratio of 10. We now use a fine 90×900 mesh to reduce the interior errors.

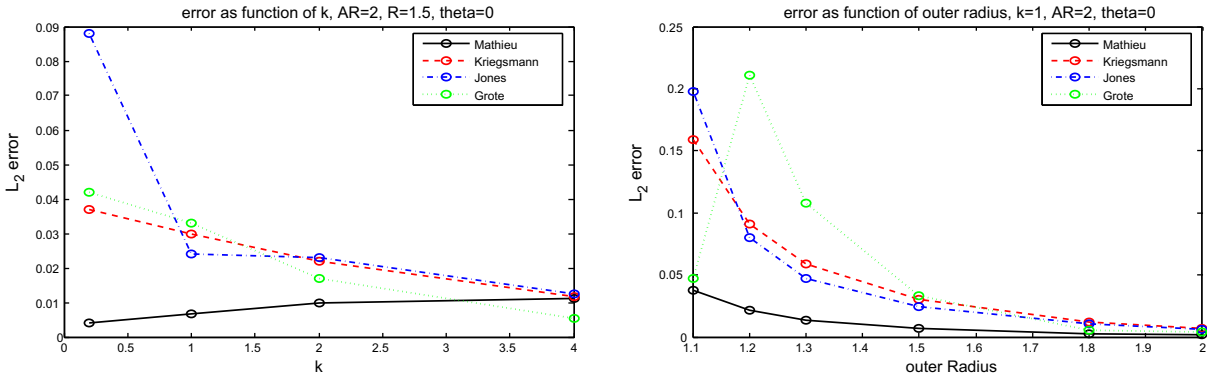

(a) dependence on k (b) dependence on outer radius

Fig. 4. L_2 error as a function of various parameters; Neumann bc.

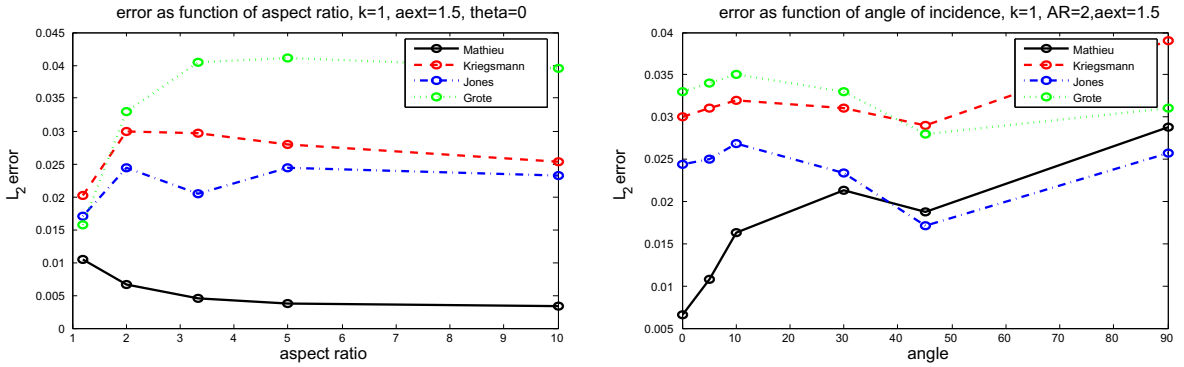

(a) dependence on aspect ratio (b) dependence on angle of incidence

Fig. 5. L_2 error as a function of various parameters; Neumann bc.

Table 5
FEM: relative error for the solution on the inner ellipse

Ellipse (1, 0.5)	$k = 0.2$	$k = 1$	$k = 2$	$k = 4$
Kriegsmann	7.9×10^{-2}	1.0×10^{-2}	9.7×10^{-3}	1.1×10^{-2}
Jones	2.1×10^{-1}	2.8×10^{-2}	1.0×10^{-2}	1.1×10^{-2}
Antoine	1.2×10^{0}	3.8×10^{-2}	1.0×10^{-2}	1.1×10^{-2}
Kallivokas	7.2×10^{-2}	2.3×10^{-2}	9.7×10^{-3}	1.1×10^{-2}
Reiner	5.9×10^{-2}	1.0×10^{-1}	1.1×10^{-1}	9.1×10^{-2}
Grote	6.0×10^{-2}	3.0×10^{-2}	1.6×10^{-2}	5.2×10^{-3}
Mathieu	2.1×10^{-3}	7.0×10^{-3}	8.9×10^{-3}	1.3×10^{-2}

Similar to the finite difference method the new modal approach (27) is best followed by that of Kriegsmann et al. (16). Including additional curvature terms only made the error larger. It is possible that the curvature terms become important if more accurate methods than a linear finite element is used. For large k all the methods gave similar results except for that of Reiner et al. (14) which was less accurate. Similar conclusions were reached for these boundary conditions used as on surface radiation conditions (OSRC) [37].

The FEM errors are generally larger than the FD ones. We assume that this occurs since the FD calculation is in elliptical coordinates while the FEM calculation uses polar coordinates. Hence, the elliptical scatterer is only approximated within the FEM code. There are similar errors at the outer elliptical surface even though the integration is carried out on the artificial elliptical surface. Occasionally the FFP error was considerably smaller than the error in the solution itself on the inner boundary. This occurs because of cancellations in the integral for the far field pattern. So the small inaccuracies in representing the ellipse in polar coordinates has a greater effect on the error in the solution than the integrated FFP error.

Table 6
FEM: relative error for the FFP, AR = 2, $b = 1.5$

Ellipse (1, 0.5)	$k = 0.2$	$k = 1$	$k = 2$	$k = 4$
Kriegsmann	1.9×10^{-3}	1.7×10^{-3}	3.7×10^{-3}	4.1×10^{-3}
Jones	7.1×10^{-2}	1.3×10^{-2}	4.3×10^{-3}	4.2×10^{-3}
Antoine	3.7×10^{-1}	1.7×10^{-2}	5.0×10^{-3}	4.2×10^{-3}
Kallivokas	2.0×10^{-2}	1.1×10^{-2}	3.6×10^{-3}	4.1×10^{-3}
Reiner	1.9×10^{-2}	2.6×10^{-2}	8.3×10^{-2}	7.4×10^{-2}
Grote	1.2×10^{-2}	1.3×10^{-2}	9.5×10^{-3}	4.7×10^{-3}
Mathieu	4.8×10^{-5}	1.1×10^{-3}	2.9×10^{-3}	4.0×10^{-3}

Table 7
FEM: relative error for the FFP, AR = 2, $b = 1.1$

Ellipse (1, 0.5)	$k = 0.2$	$k = 1$	$k = 2$	$k = 4$
Kriegsmann	1.8×10^{-2}	1.7×10^{-2}	2.8×10^{-2}	3.4×10^{-2}
Jones	2.1×10^{-1}	1.7×10^{-1}	5.2×10^{-2}	3.4×10^{-2}
Antoine	1.8×10^{-1}	2.5×10^{-1}	7.1×10^{-2}	3.5×10^{-2}
Kallivokas	1.8×10^{-1}	1.0×10^{-1}	4.2×10^{-2}	3.3×10^{-2}
Reiner	8.7×10^{-2}	1.1×10^{-1}	1.3×10^{-1}	1.7×10^{-1}
Grote	1.4×10^{-1}	1.3×10^{-1}	1.6×10^{-1}	7.4×10^{-2}
Mathieu	2.4×10^{-4}	6.8×10^{-3}	1.9×10^{-2}	3.6×10^{-2}

Table 8
FEM: relative error for the FFP, AR = 10, $b = 1.5$, 90×900 mesh

Ellipse (1, 0.5)	$k = 0.2$	$k = 1$	$k = 2$	$k = 4$
Kriegsmann	3.4×10^{-4}	4.3×10^{-4}	1.3×10^{-3}	2.3×10^{-3}
Jones	6.2×10^{-2}	1.8×10^{-2}	2.7×10^{-3}	2.6×10^{-3}
Antoine	1.2×10^{-1}	2.3×10^{-2}	3.1×10^{-3}	2.6×10^{-3}
Kallivokas	1.9×10^{-2}	1.4×10^{-2}	2.3×10^{-3}	2.5×10^{-3}
Reiner	3.7×10^{-3}	6.7×10^{-3}	3.2×10^{-2}	4.3×10^{-2}
Grote	3.0×10^{-3}	4.5×10^{-3}	3.3×10^{-3}	3.2×10^{-3}
Mathieu	7.8×10^{-5}	6.9×10^{-5}	8.5×10^{-4}	1.7×10^{-3}

4. Conclusion

In conclusion, the new modal based boundary condition (27) is superior to the others when used both for finite difference and finite element methods especially for lower frequencies. It remains accurate for high aspect ratios and high angles of incidence (not shown). Similar conclusions were previously reached for the OSRC approach [37]. For the ABCs based on various expansions the addition of curvature terms does not improve the accuracy and complicates the formulae. Hence, the ABC of Kriegsmann et al. is the next most appropriate.

Acknowledgments

Eli Turkel would like to thank the Flemish Academic Centre for Science and the Arts (VLAC) for hosting him during the research on this paper.

Appendix. Comment on symmetry of ABC for finite element computations

In this appendix, we comment on the implementation of the absorbing boundary condition when using finite elements. We divide the ABCs into two categories.

The first set consists of the boundary conditions of Givoli-Keller (13), Reiner et al. (14), and the modal condition (27). These can all be expressed in the form

$$h_\xi \frac{\partial u}{\partial n} = \frac{\partial u}{\partial \xi} = Au + B\frac{\partial^2 u}{\partial \eta^2} \tag{34}$$

with B constant. After multiplication by a test function v and integration over Σ, we need to compute the integral

$$I = \int_\Sigma \frac{\partial u}{\partial n}(\mathbf{x}) v(\mathbf{x}) \mathrm{d}\sigma(\mathbf{x}),$$

where Σ is the outer ellipse with semi-axes (a, b). We parametrize Σ with the elliptical angular coordinate η:

$$x(\eta) = a\cos(\eta t) \quad y(\eta) = b\sin(\eta).$$

The integral I becomes

$$I = \int_0^{2\pi} \frac{\partial u}{\partial n}(\mathbf{x}(\eta))v(\mathbf{x}(\eta))h_\xi \mathrm{d}\eta = \int_0^{2\pi} Au(\mathbf{x}(\eta))v(\mathbf{x}(\eta))\mathrm{d}\eta + \int_0^{2\pi} B\frac{\partial^2 u}{\partial \eta^2}(\mathbf{x}(\eta))v(\mathbf{x}(\eta))\mathrm{d}\eta \tag{35}$$

and, after integration by parts,

$$I = \int_0^{2\pi} Au(\mathbf{x}(\eta))v(\mathbf{x}(\eta))\mathrm{d}\eta - \int_0^{2\pi} B\frac{\partial u}{\partial \eta}(\mathbf{x}(\eta))\frac{\partial v}{\partial \eta}(\mathbf{x}(\eta))\mathrm{d}\eta.$$

This last relation shows that the integral I is symmetric as a function of u and v.

The second set consists of the boundary conditions of Kriegsmann et al. (16), Jones (18), Antoine et al. (19), and Kallivokas et al. (20). All these conditions have the form

$$\frac{\partial u}{\partial n} = Au - \frac{\partial}{\partial s}\left(B\frac{\partial}{\partial s}\right)$$

or

$$h_\xi \frac{\partial u}{\partial n} = \frac{\partial u}{\partial \xi} = h_\xi Au - \frac{\partial}{\partial \eta}\left(\frac{B}{h_\xi}\frac{\partial}{\partial \eta}\right). \tag{36}$$

The expression for I is now

$$I = \int_0^{2\pi} h_\xi Au(\mathbf{x}(\eta))v(\mathbf{x}(\eta))\mathrm{d}\eta - \int_0^{2\pi} \frac{\partial}{\partial \eta}\left(\frac{B}{h_\xi}\frac{\partial u}{\partial \eta}(\mathbf{x}(\eta))\right)v(\mathbf{x}(\eta))\mathrm{d}\eta$$

and, after integration by parts,

$$I = \int_0^{2\pi} h_\xi Au(\mathbf{x}(\eta))v(\mathbf{x}(\eta))d\eta + \int_0^{2\pi} \frac{B}{h_\xi}\frac{\partial u}{\partial \eta}(\mathbf{x}(\eta))\frac{\partial v}{\partial \eta}(\mathbf{x}(\eta))\mathrm{d}\eta.$$

Here, again, the integral I is symmetric with respect to u and v. Antoine [3] has shown that for a finite element method the symmetric form is more accurate.

References

[1] J.D. Angelo, I.D. Mayergoyz, On the use of local absorbing boundary conditions for RF scattering problems, IEEE Trans. Ant. Prop. 25 (1989) 3040–3042.
[2] X. Antoine, H. Barucq, A. Bendali, Bayliss–Turkel like radiation conditions on surfaces of arbitrary shape, J. Math. Anal. Appl. 229 (1999) 184–211.
[3] X. Antoine, Fast approximate computation of a time-harmonic scattered field using the on-surface radiation condition method, IMA J. Appl. Math 66 (2001) 83–110.
[4] X. Antoine, M. Darbas, Y.Y. Lu, An improved surface radiation condition for high-frequency acoustic scattering problems, Comput. Meth. Appl. Mech. Eng. 195 (2005) 4060–4074.
[5] X. Antoine, Advances in the on-surface radiation condition method: theory, numerics and applications, in: F. Magoules (Ed.), Computational Methods for Acoustics Problems, Saxe-Coburg Publication, UK, 2008.
[6] H. Barucq, R. Djellouli, A. Saint-Guirons, Two-dimensional approximate local DtN boundary conditions for elliptical-shaped boundaries, Special Issue of the 8th International Conference on Theoretical and Computational Acoustics, (ICTCA 2007), Heraklion, Crete, in press.
[7] H. Barucq, R. Djellouli, A. Saint-Guirons, Three-dimensional approximate local DtN boundary conditions for prolate spheroid boundaries, J. Comput. Appl. Math., special issue for Waves, in press.
[8] A. Bayliss, E. Turkel, Radiation boundary conditions for wave-like equations, Commun. Pure Appl. Math. 33 (1980) 707–725.
[9] A. Bayliss, M. Gunzburger, E. Turkel, Boundary conditions for the numerical solution of elliptic equations in exterior regions, SIAM J. Appl. Math. 42 (1982) 430–451.
[10] A. Bayliss, C.I. Goldstein, E. Turkel, On accuracy conditions for the numerical computation of waves, J. Comput. Phys. 59 (1985) 396–404.
[11] G. Ben-Porat, D. Givoli, Solution of unbounded domain problems using elliptic artificial boundaries, Commun. Numer. Meth. Eng. 11 (1995) 735–741.
[12] D.C. Calvo, M.D. Collins, D.K. Dalco, A higher-order on-surface radiation condition derived from an analytic representation of a Dirichlet-to-Neumann map, IEEE Trans. Ant. Prop. 51 (2003) 1607–1614.
[13] D.C. Calvo, A wide-angle on-surface radiation condition applied to scattering by spheroids, J. Acoust. Soc. Am. 116 (2004) 1549–1558.
[14] F.R. Cooray, G.I. Costache, An overview of absorbing boundary conditions, J. Electromag. Waves Appl. 5 (1991) 1041–1054.
[15] A. Ditkowski, D. Gottlieb, On the Engquist Majda absorbing boundary conditions for hyperbolic systems, Contemp. Math. 330 (2003) 55–71.
[16] R. Djellouli, C. Farhat, A. Macedo, R. Tezaur, Finite element solution of two-dimensional acoustic scattering problems using arbitrarily shaped convex artificial boundaries, J. Comput. Acoust. 8 (2000) 81–99.
[17] B. Engquist, A. Majda, Absorbing boundary conditions for the numerical simulation of waves, Math. Comp. 31 (1977) 629–651.
[18] C.I. Goldstein, A finite element method for solving Hemholtz type equations in waveguides and other unbounded domains, Math. Comp. 39 (1982) 309–324.
[19] M.J. Grote, J.B. Keller, On nonreflecting boundary conditions, J. Comput. Phys. 122 (1995) 231–243.
[20] M.J. Grote, J.B. Keller, Nonreflecting boundary conditions for Maxwell's equations, J. Comput. Phys. 139 (1998) 327–342.
[21] T. Hagstrom, S.I. Hariharan, R.C. MacCamy, On the accurate long-time solution of the wave equation in exterior domains: asymptotic expansions and corrected boundary conditions, Math. Comput. 63 (1994) 507–539.
[22] T. Hagstrom, T. Warburton, A new auxiliary variable formulation of high-order local radiation boundary conditions: corner compatibility conditions and extensions to first order systems, Wave Motion 39 (2004) 327–338.
[23] L. Halpern, R. Rauch, Error analysis for absorbing boundary conditions, Numer. Math. 51 (1987) 459–467.

[24] L. Halpern, L.N. Trefethen, Wide-angle one-way wave equations, J. Acoust. Soc. Amer. 84 (1984) 1397–1404.
[25] I. Harari, R. Djellouli, Analytical study of the effect of wave number on the performance of local absorbing boundary conditions for acoustic scattering, Appl. Numer. Math. 50 (2004) 15–47.
[26] U. Hetmaniuk, Stability estimates for a class of Helmholtz problems, Commun. Math. Sci. 5 (2007) 665–678.
[27] R.L. Higdon, Absorbing boundary conditions for difference approximations to the multi-dimensional wave equation, Math. Comp. 47 (1986) 437–459.
[28] D.S. Jones, Surface radiation conditions, IMA J. Appl. Math. 41 (1988) 21–30.
[29] D.S. Jones, An improved surface radiation condition, IMA J. Appl. Math. 48 (1992) 163–193.
[30] D.S. Jones, G.A. Kriegsmann, Note on surface radiation conditions, SIAM J. Appl. Math. 50 (1990) 559–568.
[31] L.F. Kallivokas, J. Bielak, R.C. MacCamy, A simple impedance-infinite element for the finite element solution of the three dimensional wave equation in unbounded domains, Comput. Meth. Appl. Mech. Eng. 147 (1997) 235–262.
[32] L.F. Kallivokas, S. Lee, Local absorbing boundaries of elliptical shape for scalar waves, Comput. Meth. Appl. Mech. Eng. 193 (2004) 4979–5015.
[33] G.A. Kriegsmann, A. Taflove, K.R. Umashankar, A new formulation of electromagnetic scattering using on surface radiation condition approach, IEEE Trans. Ant. Prop. AP35 (1987) 153–161.
[34] Y. Li, Z.J. Cendes, Modal expansion absorbing boundary conditions for two-dimensional electromagnetic scattering, IEEE Trans. Magn. 29 (1993) 1835–1838.
[35] B. Lichtenberg, K.J. Webb, D.B. Meade, A.F. Peterson, Comparison of two-dimensional conformal local radiation boundary conditions, Electromagnetics 16 (1996) 359–384.
[36] D.B. Meade, G.W. Slade, A.F. Peterson, K.J. Webb, Comparison of local radiation boundary conditions for the scalar Helmholtz equation with general boundary shapes, IEEE Trans. Ant. Prop. 43 (1995) 6–10.
[37] M. Medvinsky, E. Turkel, On surface radiation conditions for an ellipse, J. Comput. Appl. Math., special issue for Waves, in press.
[38] R.C. Reiner, R. Djellouli, I. Harari, The performance of local absorbing boundary conditions for acoustic scattering from elliptical shapes, Comput. Meth. Appl. Mech. Eng. 195 (2006) 3622–3665.
[39] J.J. Shirron, I.M. Babuska, A comparison of approximate boundary conditions and infinite elements for exterior Helmholtz problems, Comput. Meth. Appl. Mech. Eng. 164 (1998) 121–139.
[40] M. Teymur, A note on higher-order surface radiation conditions, IMA J. Appl. Math. 57 (1996) 137–163.
[41] R. Tezaur, A. Macedo, C. Farhat, R. Djellouli, Three-dimensional finite element calculations in acoustic scattering using arbitrarily shaped convex artificial boundaries, Int. J. Numer. Meth. Eng. 53 (2002) 1461–1476.
[42] L.L. Thompson, R. Huan, C. Ianculescu, Finite element formulation of exact Dirichlet–Neumann radiation conditions on elliptic and spheroidal boundaries, in: Proc. IMECE'99, ASME, 1999.
[43] E. Turkel, C. Farhat, U. Hetmaniuk, Improved accuracy for the Helmholtz equation in unbounded domains, Int. J. Numer. Meth. Eng. 59 (2004) 1963–1988.
[44] E. Turkel, Boundary conditions and iterative schemes for the Helmholtz equation in unbounded regions, in: F. Magoules (Ed.), Computational Methods for Acoustics Problems, Saxe-Coburg Publication, UK, 2008.
[45] B. Yilmaz, The performance of the higher-order radiation condition method for the penetrable cylinder, Math. Prob. Eng., vol. 2007, Article ID 17605, 14 p., 2007.